IMPERIAL

Concrete Trials 2

CCUS Innovation 2.0

Key Knowledge Deliverable 3.3

October 2024

Key Knowledge Deliverable Cover Sheet

This Key Knowledge Deliverable (KKD) has been produced by Imperial College London as part of the Department for Energy Security and Net Zero £1bn Net Zero Innovation Portfolio (NZIP) - CCUS Innovation 2.0 programme. The document is reflective of the status of the project at the time of writing. The material presented could have been subject to change as the project matured. These documents should not be considered a full representation of the final project.

Project Description

This project seeks to further develop and scale a new carbon sequestration process which transforms waste CO2 gas from industrial facilities into valuable construction products. Sequestered CO2 through this process is cheaper than conventional approaches that rely on purification, liquification and offshore or geological storage. The CO2 is stored in the form of a stable mineral which ensures they will be no leakage over time.

The patent-pending technology involves taking globally abundant magnesium silicate minerals and splitting this into magnesia and silica components. Through simple chemical processing two products of high purity are created: a) an amorphous silica that can be used as supplementary cementitious material (SCM) to facilitate low-carbon concrete and b) a concentrated magnesium solution in which CO2 from industrial flues can be sequestered to produce other construction materials.

This CCUS Innovation 2.0 award will be used to increase our technology and commercial readiness level by de-risking and facilitating the development of a pilot facility, in order to demonstrate that the technology is economically viable and deployable at scale.

Description of KKD

Report detailing progress update on concrete testing, and intermediate results. The exact scope of this will be determined by D3.2.

KKDs to be released in full

- D3.4 – Concrete Trials 3
- D4.4 – Product Optimisation 2

KKDs to be released after redactions

- D1.1 – Flue Gas Recovery and Testing 1
- D1.2 – Dissolution Procurement
- D1.3 – Dissolution Operation
- D1.4 – Flue Gas Recovery and Testing 2 & Carbonation Procurement
- D1.5 – Carbonation Operation
- D2.3 – Reagent Regeneration Procurement
- D2.4 – Reagent Regeneration Operation
- D3.2 – Concrete Trials 1
- D3.3 – Concrete Trials 2
- D4.2 – Process Optimisation
- D4.3 – Product Optimisation 1
- D5.2 – Business Development 2 (Supply Chain)
- D5.3 – Business Development 3 (Business Planning)
- D5.4 - Business Development 4 (Commercial Readiness)
- D6.1 – Year 1 Report
- D6.2 – Year 2 Report

Any enquiries regarding this publication should be sent to us at:
nzip@energysecurity.gov.uk

Contents

Summary 6
Introduction 7
Methods 8
Materials preparation and characteristics 8
Pozzolanic reactivity 11
Hydration mechanisms 11
Mortar preparation and characterization 12
Results and discussion 15
Pozzolanic reactivity of recovered silica 15
Influence of silica and sulfate content on hydration kinetics 15
Hydration products 17
Phase assemblage and degree of hydration 17
Thermogravimetry analysis 21
Influence of silica on water demand and workability 24
Compressive strength 25
Conclusions 27

Summary

This deliverable looked at how silica produced from the acid digestion of olivine can be used as a cement substitute in concrete. In this report, cement was replaced with up to 40% of olivine-derived silica and the gypsum addition was adjusted to improve performance. The work has investigated how silica reacts with cement phases, and how it influenced concrete strength over time. The results revealed that the silica is highly reactive, it reacts rapidly, and it has a large surface area. This accelerates the hardening process and significantly increases concrete strength. The compressive strength of the concrete was over 50 MPa after hydrating for 90 days. This is marginally lower than regular concrete but adding a small amount of gypsum (up to 3-4wt.%) improves the early strength. The high specific surface area of olivine-derived silica increases the water demand of blended cement. It was found that a maximum water-to-cementitious binder ratio of 0.63 could be used without affecting the compressive strength of blended cement mortars. This was for a maximum of 20 wt.% replacement, beyond which strength significantly decreases. This study demonstrates that silica derived from olivine is a promising SCM for producing concrete that has comparable performance to normal concrete, but which is associated with reduced carbon emissions.

Introduction

Carbon capture and storage/utilization (CCSU) is an approach being implemented to reach net zero in cement production. This generally involves capturing carbon released from the kiln, followed by geological sequestration (CCS) or conversion into valuable products (CCU). This research is developing a novel process involving acid digestion of olivine, a globally abundant magnesium silicate mineral, followed by CO2 sequestration through mineralization to form magnesium carbonate. As part of the process, the olivine-derived silica has been characterized and tested as an SCM (deliverable reports 3.1 and 3.2). It has been shown that olivine-derived silica significantly reduces the rheological properties of blended cement due to the high specific surface area. The lower compressive strength observed was due to the difficulty in properly mixing the silica, rather than the reactivity as an SCM. This deliverable investigated the complex interactions between the olivine-derived silica and cement hydration. The aim was to understand the mechanisms by which this SCM influences the formation of cement hydration products and the compressive strength of cementitious materials. The objective is to determine the optimum condition for using olivine-derived silica in high-performance, sustainable, concrete.

Methods

Materials preparation and characteristics

Portland cement of class CEM I 52.5R was used with silica recovered from olivine as an SCM. Commercial grade gypsum ($CaSO_4.2H_2O$, 99 % purity) from VWR was used as a sulfate carrier to regulate hydration. The silica was prepared following the procedure described by Shanks et al. [1]. The process involves the digestion of olivine $(Mg, Fe)_2SiO_4$, supplied by Sibelco Nordic AS) in sulfuric acid (H_2SO_4, 98 wt%, from VWR) at 70 ºC for 2 hours. In this work, a ratio of 200g of olivine to 1 L of 3M sulfuric acid solution was used. Isopropanol (IPA, 99 wt%, Sigma-Aldrich) was then added to the bulk solution for liquid-liquid phase separation. After phase segregation, the solid part consisting of silica was removed using a 0.5 mm sieve. The recovered silica was dried at 70 ºC to remove excess IPA and washed to eliminate contaminants. The final stage consisted of drying the silica at 105 ºC to remove as much free water as possible. Use the Return key to continue numbering.

Table 1 shows the chemical composition and physical properties of olivine-derived silica and Portland cement. The chemical composition was measured by using X-ray fluorescence (XRF, Malvern Panalytical Zetium). The specific surface area of raw materials was determined using nitrogen adsorption (Micromeritics 3Flex), and the density was determined using a Helium pycnometer (Micromeritics AccuPyc II 1340). The particle size distribution data was obtained using laser scattering (Malvern Mastersizer 3000) with water as a dispersant. The XRD data of silica and a backscattered scanning electron microscopy image (Hitachi TM4000 plus) are shown in Fig 1. The mineralogical composition of the olivine-derived silica and Portland cement was determined using a Malvern Panalytical Empyrean XRD as presented in Table 2. The silica is rich in SiO_2 (73 wt.%). The 15 wt.% of LOI corresponds to the dehydroxylation of silanol groups and unreacted minerals in olivine on heating to 1050 ºC for 2 hours. The silica is amorphous but contains clinochlore ($Mg_5Al(AlSi_3O_{10})(OH)_8$) and chabazite $(Ca,K_2,Na_2)_2[Al_2Si_4O_{12}]2.12H_2O$) as mineral phases associated with unreacted olivine. The silica is porous and forms an agglomerated gel, with particles having mean diameters of 40.6 µm.

Figure 1 X-ray patterns of silica (top) and BSE image of silica (bottom)

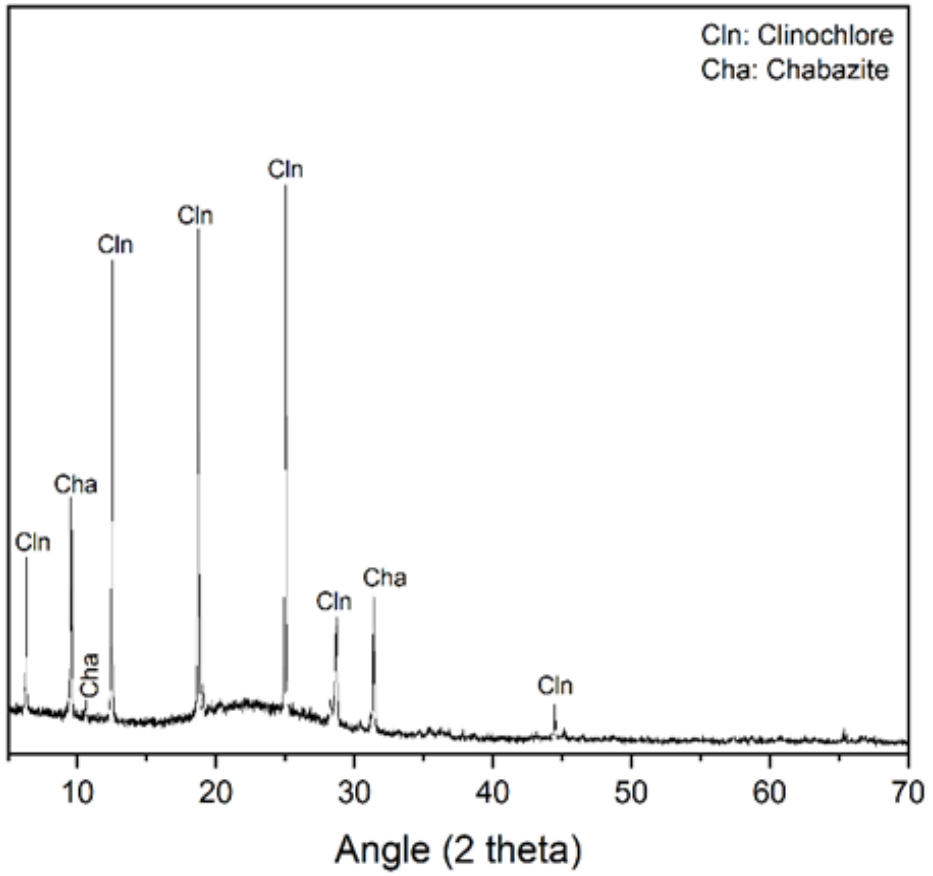

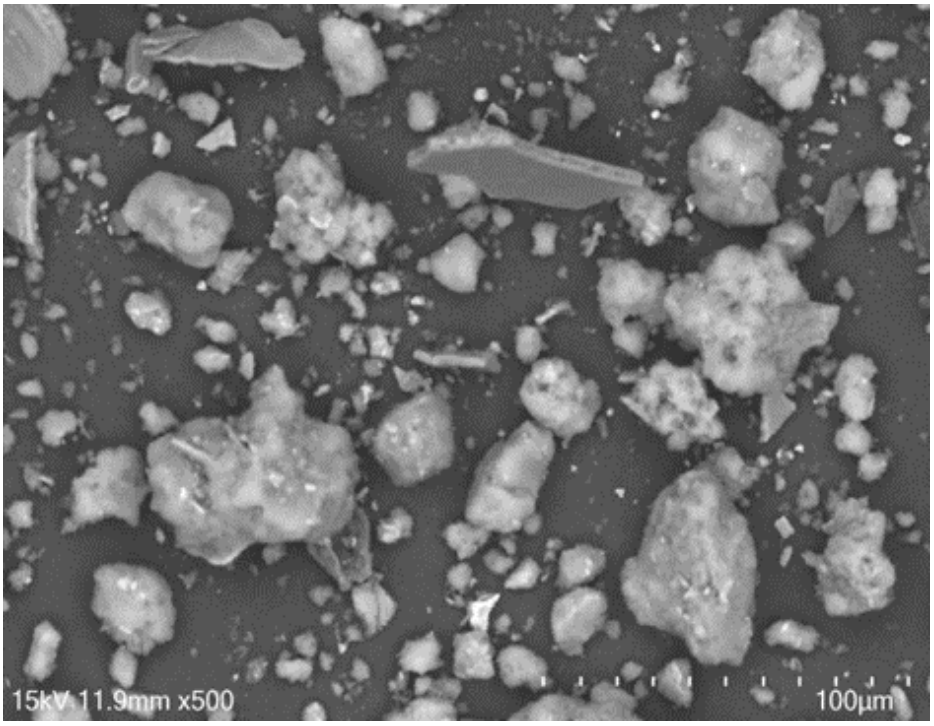

Table 1 Chemical composition of the olivine-derived silica and CEM I

Composition (%)										
Oxide	SiO2	Al2O3	MgO	CaO	Fe2O3	SO3	Cr2O3	Na2O	LOI	Sum
silica	73.1	1.07	3.35	0.49	1.89	4.00	0.85		15	99.8
CEM I	20.3	6.08	1.31	62.1	2.67	3.49	-		1.94	97.8

Table 2 Mineralogical composition of Olivine, silica and CEM I from quantitative XRD

Phase	ICSD	Content (%)		
		Olivine	silica	CEM I
Clinochlore	98-016-4234	18.4	32.3	-
Chabazite	98-002-3913	7.0	14.6	-
Forsterite	98-008-5312	67.0	-	-
Biotite	98-009-5359	2.8	-	-
Lizardite	98-002-3813	4.2	-	-
Montmorillonite	98-016-1171	0.6	-	-
Alite, C3S	98-002-2501	-	-	60.9
Belite, C2S	98-024-5077	-	-	8.7
Tricalcium aluminate, C3A	98-015-1369	-	-	5.0
Brownmillerite, C4AF	98-005-1266	-	-	1.0
Quartz	98-004-1447	-	-	1.1
calcite	98-008-8029	-	-	1.6
Anhydrite	98-005-6107	-	-	1.2
Amorphous	-	-	53.2	20.8

Pozzolanic reactivity

The pozzolanic reactivity of the olivine-derived silica was measured using the R3 test method. For this, a paste consisting of 10 g of silica, 30g Ca(OH)2, 5g of CaCO3 and 54g of potassium solution (4g/L KOH+20g/L K2SO4) was used, as defined in ASTM standard C1897-20 [1]. 50g of paste was fed in a 125 ml ampoule and placed in the TA instruments (TAM Air 3-channel) set at 40°C. This was chosen to ensure that the thermal signal was within the detection range of the calorimeter. A further 31.25 g of water was used as the reference to have the same ratio of 15g (paste)/ (9.40 g reference) of the standard. Three repeated measurements were recorded to calculate the final cumulative heat release per gram of silica as defined by ASTM C1897-20. Thermogravimetric analysis of hydrated R3 paste at 3 and 7 days was also completed using a Netzsch STA 449 F5 Jupiter, under an inert atmosphere of N2 flowing at a rate of 50 mL/min over the temperature range from 40 to 1000 °C, with a heating rate of 10 K/min.

Hydration mechanisms

The approach to investigating the interactions between silica and cement during hydration includes the measurement of heat evolution at different silica and gypsum replacement rates, using an isothermal conduction calorimeter at 25 ºC (TA instruments, TAM Air 8-channel). For this test, 10 g of paste, with the mixed composition described in Table 3, was weighed into an ampoule and placed in the calorimeter. The paste was prepared by mixing different components for at least 30 seconds using a vortex mixer. Due to the high fineness of the silica, 1 wt.% of PCE-based superplasticizer (Viskoflow3000, Sika) was added to obtain a workable paste at a water-to-cementitious materials (W/CM) ratio of 0.5. Following this test, the ampoules with the pastes were kept in a sealed plastic bag to avoid carbonation until further tests were carried out at 3, 7 and 28 days. Thermogravimetric analysis was also carried out for the quantification of the CH consumption rate on the resulting paste at 3, 7 and 28 days. The mineralogy was determined using a Malvern Panalytical, Empyrean X-ray diffractometer with CuKα radiation in a 2-theta range of 5-70o and a step of 0.02o/min. The quantitative XRD was performed on hydrated cement pastes using a Rietveld analysis method with alumina as the internal standard. From the data, the degree of hydration of clinker (DoH) was calculated using equation 1. The amount of the different phases in the hydrated cement was first normalized in g/100g of anhydrous phases, before processing in the calculation of DoH.

$$\text{DoH}\ (\%) = \frac{\sum (C_3S + C_2S + C_3A + C_4AF)_i - \sum (C_3S + C_2S + C_3A + C_4AF)_f}{\sum (C_3S + C_2S + C_3A + C_4AF)_i} \qquad (1)$$

Table 3 Mix design of paste and mortar samples.

Mix	Binder (wt. %)			Water/binder ratio	Superplasticizer (wt. %)	Sand/binder ratio
	CEM I	Silica	Gypsum			
Paste						
P0	100	-	-	0.5	-	-
P10	90	10	-	0.5	1	-
P20	80	20	-	0.5	1	-
P20-2	78.4	19.6	2	0.5	1	-
P20-3	77.6	19.4	3	0.5	1	-
P20-4	76.8	19.2	4	0.5	1	-
Mortar						
M0	100	-	-	0.63	-	3
M10	90	10	-	0.63	2	3
M20	80	20	-	0.63	2	3
M40	60	40	-	0.63	2	3
M20-2	78.4	19.6	2	0.63	2	3
M20-3	77.6	19.4	3	0.63	2	3
M20-4	76.8	19.2	4	0.63	2	3

Mortar preparation and characterization

Silica has a higher SSA (146.1 m2/g) compared to cement (1.14 m2/g). This increases the water demand for achieving a workable mortar. In general, the Vicat apparatus is used to measure the water demand, taken as the water content required to achieve a certain consistency. This method relies on varying the W/CM mass ratio and it ignores the entrapped air which might overestimate the amount of water, especially when using a very fine SCM. To know the impact of silica on water demand and choose the right water-to-cementitious materials ratio, the solid concentration of paste samples of cement and cement with 30 wt.% silica using the wet packing methods was determined. This method was carried out following procedures developed in [2,3] and involved measuring the apparent density of a cement paste obtained at different W/CM volume ratios to identify the maximum packing density. The volume

ratio is used instead of the mass ratio to consider air-entrapped voids induced by the silica, knowing that voids may be filled by water and/or air during mixing. The data was used to find the void content and solid concentration. The packing density is considered as the maximum solid concentration at which the particles are tightly packed against each other. The solid concentration (Ø) and void ratio (μ) were calculated using Eqs. (2), (3) and (4).

$$V_C = \frac{M}{\rho_\alpha R_\alpha + \rho_\gamma R_\gamma + \rho_w \mu_w} \quad (2)$$

$$\mu = \frac{(V - V_C)}{V_C} \quad (3)$$

$$Ø = {}^{V_C}/_{V} \quad (4)$$

where M and V are the mass and volume of paste in the cylindrical mould respectively; ρw is the density of water, ρα and ργ the corresponding solid density of cement and silica respectively. Rα and Rγ are the volumetric ratios of cement and silica respectively. Vc, μ, and Ø are the solid volumes of the cementitious materials (cement+ silica), voids ratio, and solid concentration.

The data obtained was used to prepare mortar samples using the mix design described in Table 3. Cement, silica, and sand were mixed at a slow speed for 2 minutes to homogenize the powder. Water and superplasticizer were then added and mixed for 2 minutes at a slow speed and 3 minutes at a fast speed. The flow test of the mortar samples was measured using a flow table (Fig 2) after dropping the table for 15 seconds. The mixture was cast in 50 mm cube molds and vibrated for 3 minutes before storing it in a curing room for 24h at 99% relative humidity. Samples were then demoulded and cured under water until testing, which was carried out at 3, 7, 28, and 90 days. Compressive strength testing was performed on mortar samples (shown in Fig 3) using an Instron 5984 Series machine operating at 0.03 KN/s rate. The final value was the average of three replicated measurements.

Figure 2 Image of mortar samples during flow test

Figure 3 . Image of mortar samples used for compressive test

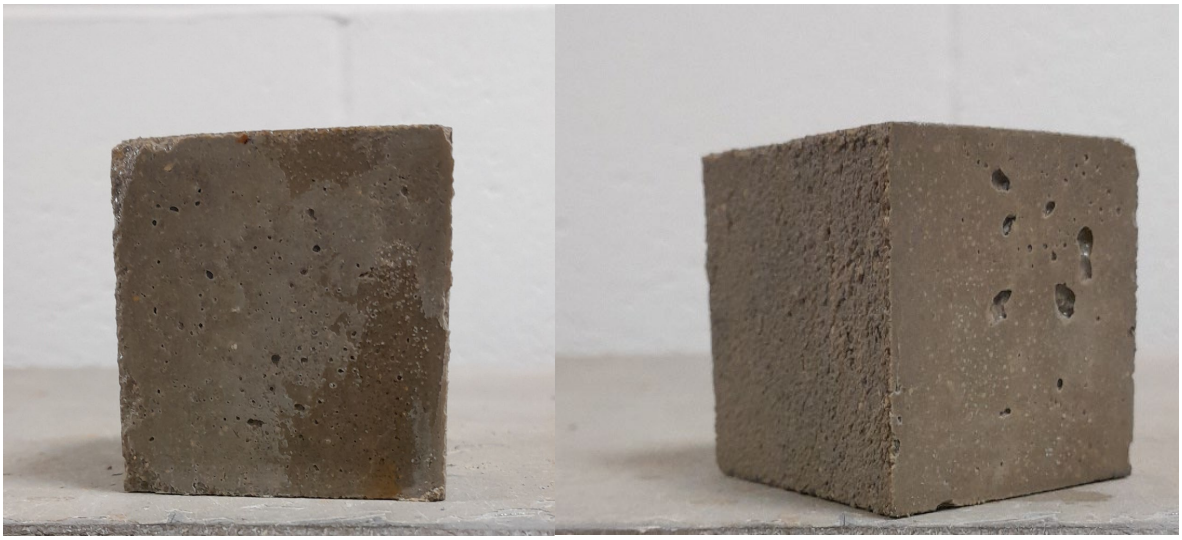

Results and discussion

Pozzolanic reactivity of recovered silica

The reactivity of silica measured from the R3 test is shown in Fig 4. The cumulative heat of the reaction increases sharply during the first 15 hours because of the rapid dissolution of the silica and calcium hydroxide/calcium carbonate. After that, the heat release slows down, and plateaus from 84 hours onward. The heat of the reaction is 315 J/gsilica after 3 days and 332 J/gsilica after 7 days. The amount of unreacted calcium hydroxide (normalized per g of initial quantity) is 47.6% and 44.2 % at 3 and 7 days respectively. The minor change in the heat of the reaction or the amount of unreacted calcium hydroxide from 3 to 7 days is driven by the pozzolanic reaction of silica with dissolved calcium. This demonstrates that the reaction rate is a maximum after 3 days, beyond which it increases only marginally. The heat of reaction is comparable to, or even higher than, that of some other pozzolanic materials such as calcined clay (300-800 J/gSCM), silica fume (360-630 J/gSCM), ground granulated blast furnace slag (240-550 J/gSCM), coal fly ash (178-294 J/gSCM) and volcanic ash (180-270 J/gSCM) [4–7]. Therefore, the silica recovered from olivine can be classified as a reactive SCM.

Figure 4 (a) Cumulative heat evolution and (b) thermogravimetry curves of the R3 paste

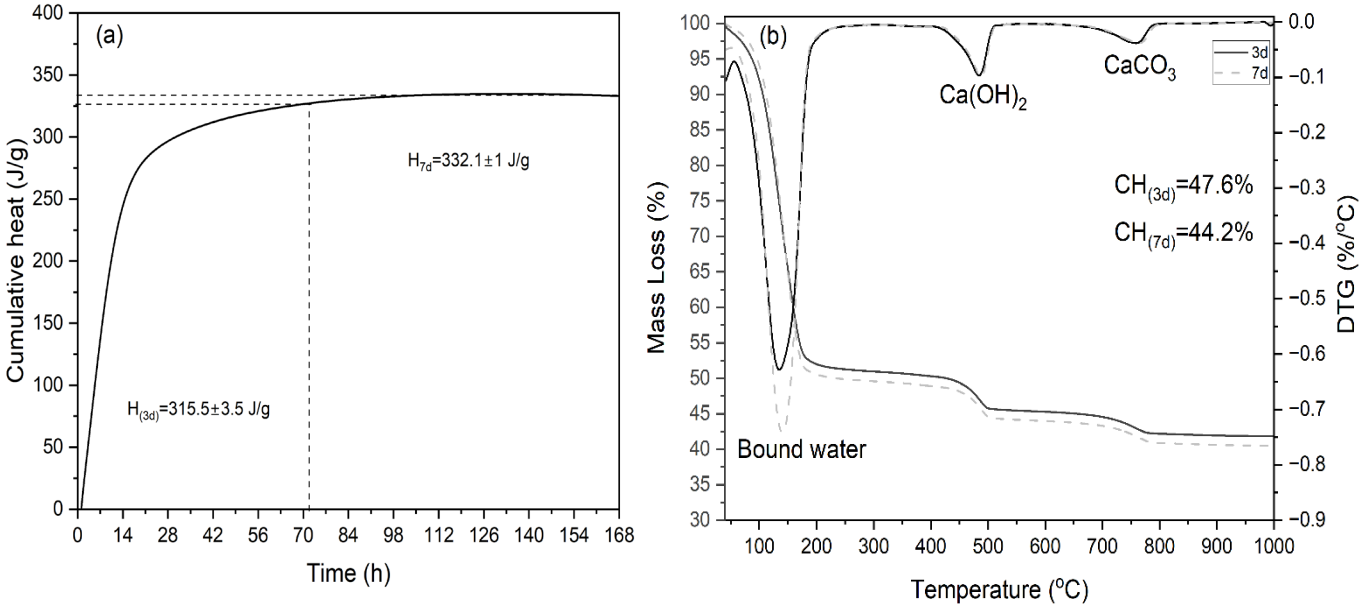

Influence of silica and sulfate content on hydration kinetics

The isothermal calorimetry results of cement and blended cement pastes with varying silica content, normalized per gram of cement are shown in Fig 5. The main hydration stage of the cement phases, alite (C3S) and aluminate (C3A), appears almost simultaneously for the sample P0. That means a congruent dissolution of alite and aluminate occurs during the cement hydration, where a high volume of C-S-H phases are formed before the hydration of aluminate initiates the setting [8]. Blending cement with silica shows a different trend, with the heat of hydration of alite appearing as a weak peak that is barely distinguishable, while the

heat of hydration of aluminate is predominant and increases with the content of silica. The time to reach the peak maximum of the heat flow for each phase is also shortened with increased silica content. The cumulative heat evolution of hydration increases with the silica content and the early onset time of dissolution of aluminate, characterized by the acceleration of the slope of the heat evolution curves occurs within the first 15h. This behaviour is commonly known as the acceleration of the sulfate depletion rate and is fostered by the increased content of the finer fraction in SCM or its dosage [9]. Sulfate depletion stems from the rapid precipitation of C-S-H due to the accelerated hydration of the C3S during the initial stage. It is suggested that the degree of hydration of C3S is linked to the onset time of the aluminate peak [10]. This is due to the higher sorption of sulfate onto C-S-H, resulting in a rapid depletion of sulfate and subsequent acceleration of aluminate hydration. As such, an increase in the rate of C-S-H precipitation at an early stage accelerates the onset of aluminate hydration during the main reaction stage. This reaction path is fostered by the filler effect and the higher specific surface area of the SCM [11]. The consequence is the flash setting of the cement paste and a reduction in workability.

Figure 5 a) Normalized heat flow and b) cumulative heat of cement pastes with 0, 10 and 20 wt.% APS at 0.5 w/b ratio.

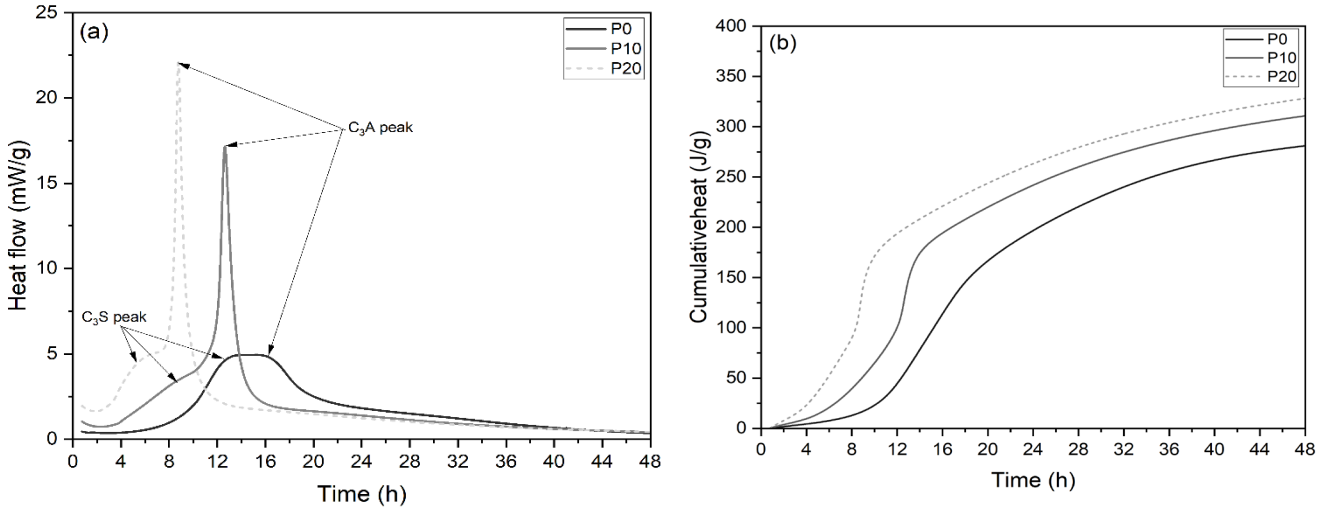

Fig 6 depicts the effect of additional gypsum (CaSO4.2H2O) on the heat of hydration of blended cement substituted with 20 wt.% silica. As expected, the aluminate hydration peak is delayed, and its intensity is greatly reduced, while the area under the peak increases. In addition, the alite peak appears later when 2 wt.% of gypsum is added. The cumulative heat (Fig 6b) displays improved features due to the effect of gypsum on the hydration of blended cement with silica. Before 5 hours of reaction time, a significant increase in the heat of hydration related to the improved dissolution of alite (C3S) occurs. From 5 hours the sample P20 shows a sharp increase of the slope of the curves, due to the enhanced dissolution of C3A as observed in Fig 6a. The slope of the curves for samples with P20-2 to P20-4 is less sharp and more flattened with the increased additional gypsum content. That means that in addition to the enhancement of the hydration rate due to the filler effect of gypsum, there is also an acceleration of the pozzolanic reaction. This helps to precipitate more C-S-H and other hydration products. The benefits of sulfate in regulating the hydration of blended cement have

been reported [12,13]. Indeed, the dissolved sulfate ions react with aluminate to retard its dissolution, allowing it to occur after the dissolution of alite.

Figure 6 Heat flow (a) and cumulative heat curves (b) of blended cement paste with 20 wt.% silica and varying additional gypsum content (2-4wt.%).

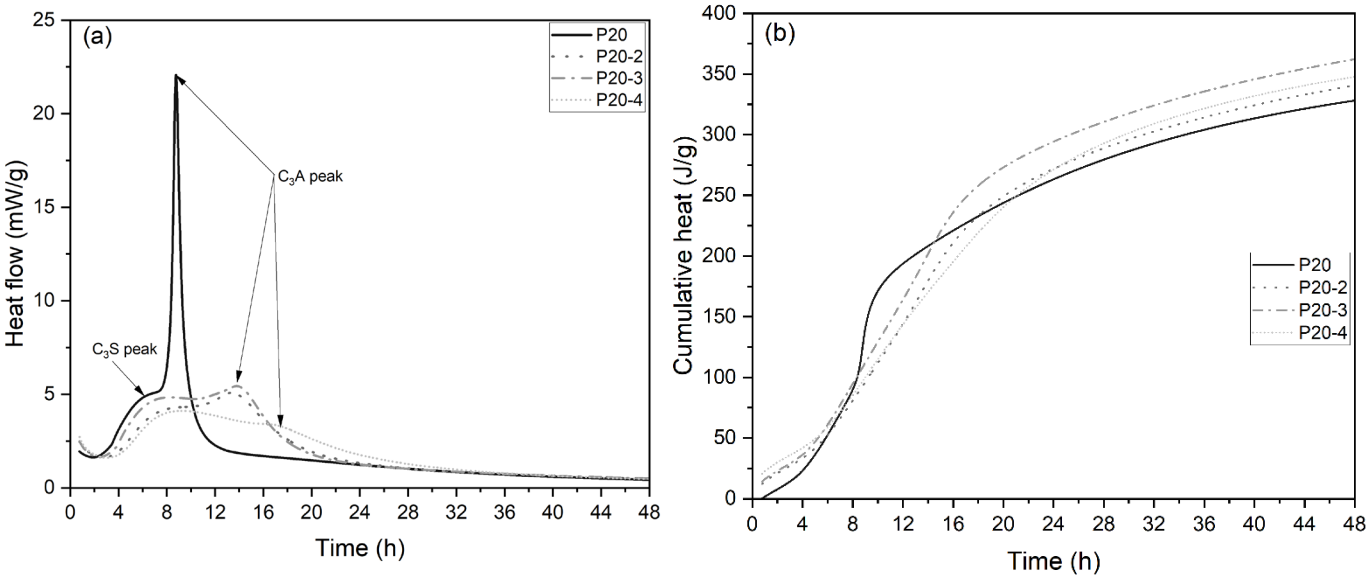

Hydration products

Phase assemblage and degree of hydration

Table 4 reports the quantitative XRD of the phase assemblage of hydrated cement with varying silica. In addition to hydrated phases, unreacted phases from cement and silica, are observed. The control sample P0 has a portlandite (calcium hydroxide, CH) content that increases with curing age. This complies with the progress of cement hydration where the dissolved calcium reacts with hydroxyl ions (-OH) in the pore solution to form calcium hydroxide, and with the dissolved silicates to form calcium silicate hydrate (C-S-H). The CH content in blended cement pastes is lower than the control and decreases significantly with the APS content at all ages. This is due to the dilution effect and pozzolanic reactivity of the APS. This can also explain the decrease of the unreacted C3S content with curing age and APS content, which is prominent at 28 days. The evolution of the amorphous content with age follows the same trend and confirms the role of silica in accelerating the formation of the CSH phase. The changes in phase assemblage with the addition of 2-4 wt.% gypsum to P20 are reported in Table 5. The CH formation seems to be less affected by sulfate adjustment. The major change involves the increased formation of ettringite (up to 18.6%) with increased gypsum content. It constitutes the main hydration product among the crystalline phases. The ettringite content increases with curing age up to 7 days, then decreases. That behaviour can be explained by the formation of different AFm phases. That is because ettringite can be transformed into monosulfate as observed in the XRD data of blended cement. When considering the hydration rate of clinker phases the evolution of the degree of hydration (DoH) is shown in Fig 7 and 8. As expected, the degree of hydration is accelerated with the silica

content at all ages and reaches up to 93% (P20) after 28 days against 85% for P0 at the same age (Fig 7). The addition of gypsum to sample P20 (Fig 8) accelerated the DoH at 3 and 7 days with limited effect at 28 days. That is ascribed to the delayed hydration of aluminates that enhanced the hydration of the alite (C3S).

Table 4 Quantitative XRD of minerals phase assemblage (%) in hydrated pastes samples with 0, 10, and 20 wt.% silica APS content at 0.5 w/b ratios cured to 28 days at different ages.

Phase	3 days			7 days			28 days		
	P0	P10	P20	P0	P10	P20	P0	P10	P20
Clinochlore	0.0	0.4	2.2	0.0	0.6	1.5	0.0	0.1	0.5
Chabazite	0.0	0.3	1.0	0.0	0.5	0.6	0.0	0.1	0.2
Portlandite	10.0	5.9	2.5	15.1	7.1	2.8	11.0	7.9	1.3
Ettringite	7.8	7.0	9.5	7.5	6.3	6.2	6.0	7.7	4.2
AFm	0.6	0.9	0.7	1.6	1.4	0.8	0.5	0.7	0.1
C3S	6.5	3.4	5.0	1.7	1.2	1.9	3.0	0.5	0.5
C2S	5.4	4.9	5.9	6.0	5.0	4.5	3.9	3.9	1.6
C3A	0.0	0.0	0.0	0.0	0.0	0.0	0.0	0.0	0.0
C4AF	0.0	0.1	0.4	0.0	0.0	0.0	0.0	0.0	0.0
Quartz	0.2	0.6	0.2	0.3	0.2	0.2	0.2	0.2	0.1
Calcite	0.8	0.7	1.6	0.7	0.4	0.9	0.4	0.9	0.5
Anhydrite	0.0	0.0	0.0	0.0	0.0	0.0	0.0	0.0	0.0
Amorphous	68.7	75.8	71	67.1	77.3	80.6	75.0	77.5	91.0

Table 5 Quantitative XRD of phase assemblage (%) of blended cement paste with 20 wt.% APS and varying additional gypsum (2-4 wt%) at content 0.5 w/b ratio cured to 28 days at different ages

Phase	3 days			7 days			28 days		
	P20-2	P20-3	P20-4	P20-2	P20-3	P20-4	P20-2	P20-3	P20-4
Clinochlore	0.7	1.1	1.4	1.0	1.0	7.3	0.4	0.3	0.9
Chabazite	0.3	0.4	0.3	0.5	1	0.9	0.3	0.4	0.4
Portlandite	1.3	1.2	0.9	1.7	1.7	4.4	1.4	1.8	1.4
Ettringite	6.4	9.0	8.1	6.3	11.5	18.6	6.6	8.8	10.4
AFm	0.5	0.3	0.1	0.6	0.5	0.1	0.1	0.0	0.0
C3S	2.5	2.5	2.4	1.2	1.7	1.5	0.4	1.5	1.1
C2S	3.7	3.2	2.3	3.2	3.9	6.1	2.3	2.7	3.0
C3A	0.0	0.0	0.0	0.0	0.0	0.0	0.0	0.0	0.1
C4AF	0.2	0.2	0.0	0.0	0.0	0.0	0.0	0.0	0.0
Quartz	0.1	0.1	0.1	0.1	0.1	0.2	0.1	0.1	0.1
Calcite	0.7	0.6	0.5	0.5	0.7	1.8	0.7	1.2	1.4
Anhydrite	0.0	0.0	0.0	0.0	0.0	0.0	0.0	0.0	0.0
Amorphous	83.6	81.4	83.9	84.9	77.9	60.1	87.9	83.2	81.2

Figure 7 Degree of hydration of clinker at varying silica content

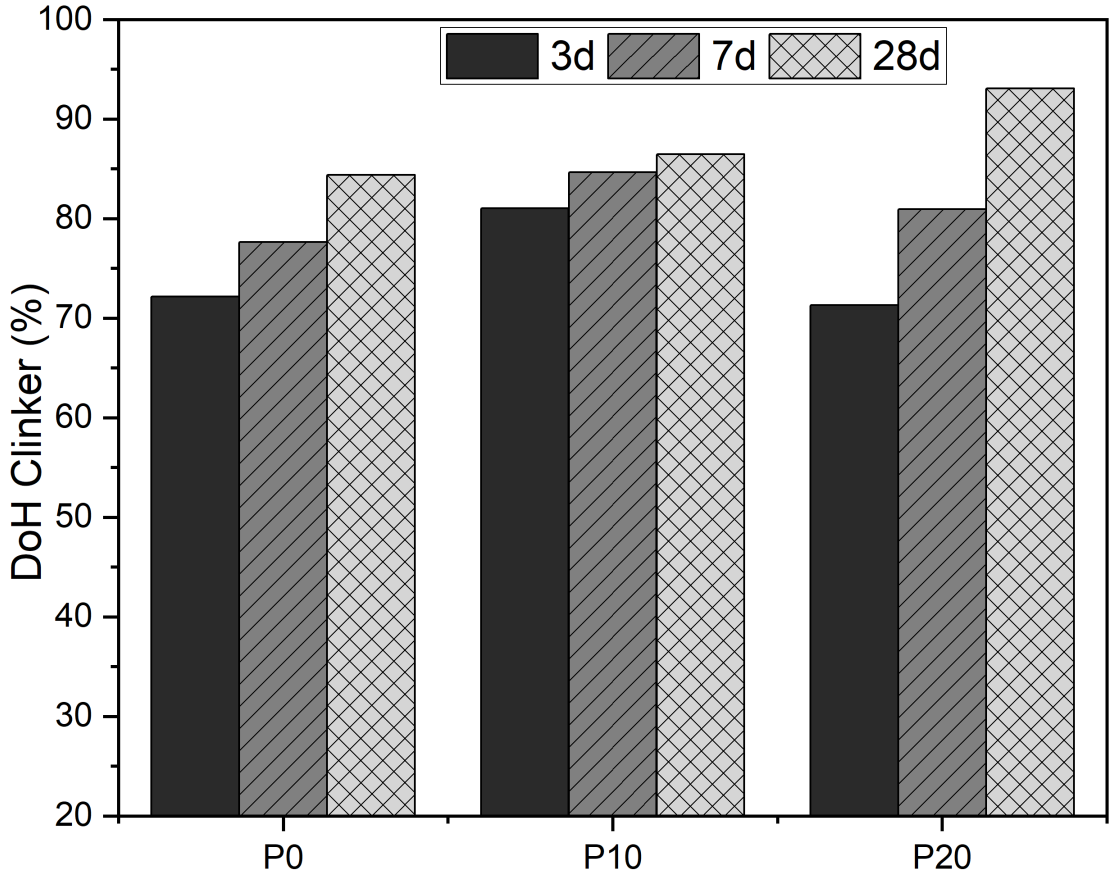

Figure 8 Degree of hydration of clinker with varying additional gypsum content for 20wt.% silica replacement

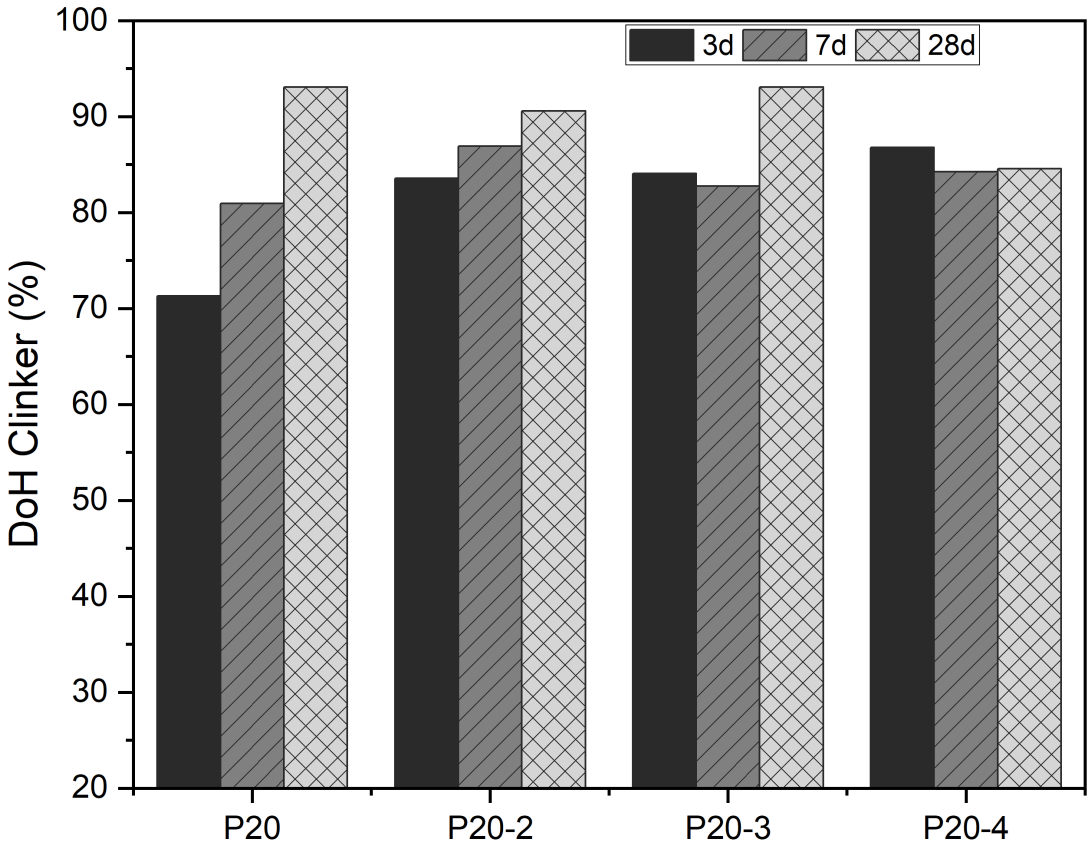

Thermogravimetry analysis

Fig. 9 shows the differential thermogravimetry (DTG) of hydrated cement pastes at 3 and 28 days with varying APS content (0-20 wt.%) and gypsum addition (0-4 wt.%) for 20 wt.% silica. The major mass loss before 250 oC corresponds to the decomposition of C-S-H, ettringite and AFm. Silica also loses water in that range coming from the free water and the condensation of the silanol group [14]. AFm is barely visible at 3 days, but by 28 days a small shoulder associated with its decomposition can be seen at ~200 oC, especially for P0 (Fig. 9a, b). The partial substitution of cement with silica decreases the formation of AFm. The addition of gypsum (Fig. 9c,d) increases mass loss associated with the decomposition of C-S-H and ettringite. The formation of AFm is impaired and barely discernable on P20-2 to P20-4. Overall, these observations agree with the fluctuations in the formation of the different AFm phases as observed in the XRD data of those samples and are related to the silica influence on hydration. Finally one can also observe the decomposition of clinochlore and chabazite from unreacted silica and the decomposition of calcite either from the carbonation of CH or the unreacted cement.

Fig. 10 highlights the unreacted CH content with time in hydrated cement with varying silica content and gypsum content for 20 wt.% silica. The tangent method was used to quantify the mass loss corresponding to the decomposition of portlandite in the temperature range 400 - 600 oC and used to calculate the CH content as described in [15]. CH content increases with time but decreases with the silica content (Figs 10a). That increase is related to the continuous hydration of the cement phases with time as described earlier. As expected CH content in blended cement decreases with silica content as a consequence of both dilution effect and pozzolanoic reaction. The CH content does not evolve proportionally with the gypsum content as the silica content in the mixes is relatively the same (Fig 10b). However, it increases with time except for mixes with 3 and 4wt.% gypsum, where it is inconsistent.

Figure 9 DTG of the control cement and blended cement paste with silica content at 3 days (a) and 28 days (b), and with varying additional gypsum content for 20wt.% silica content at 3 days (c) and 28 days (d).

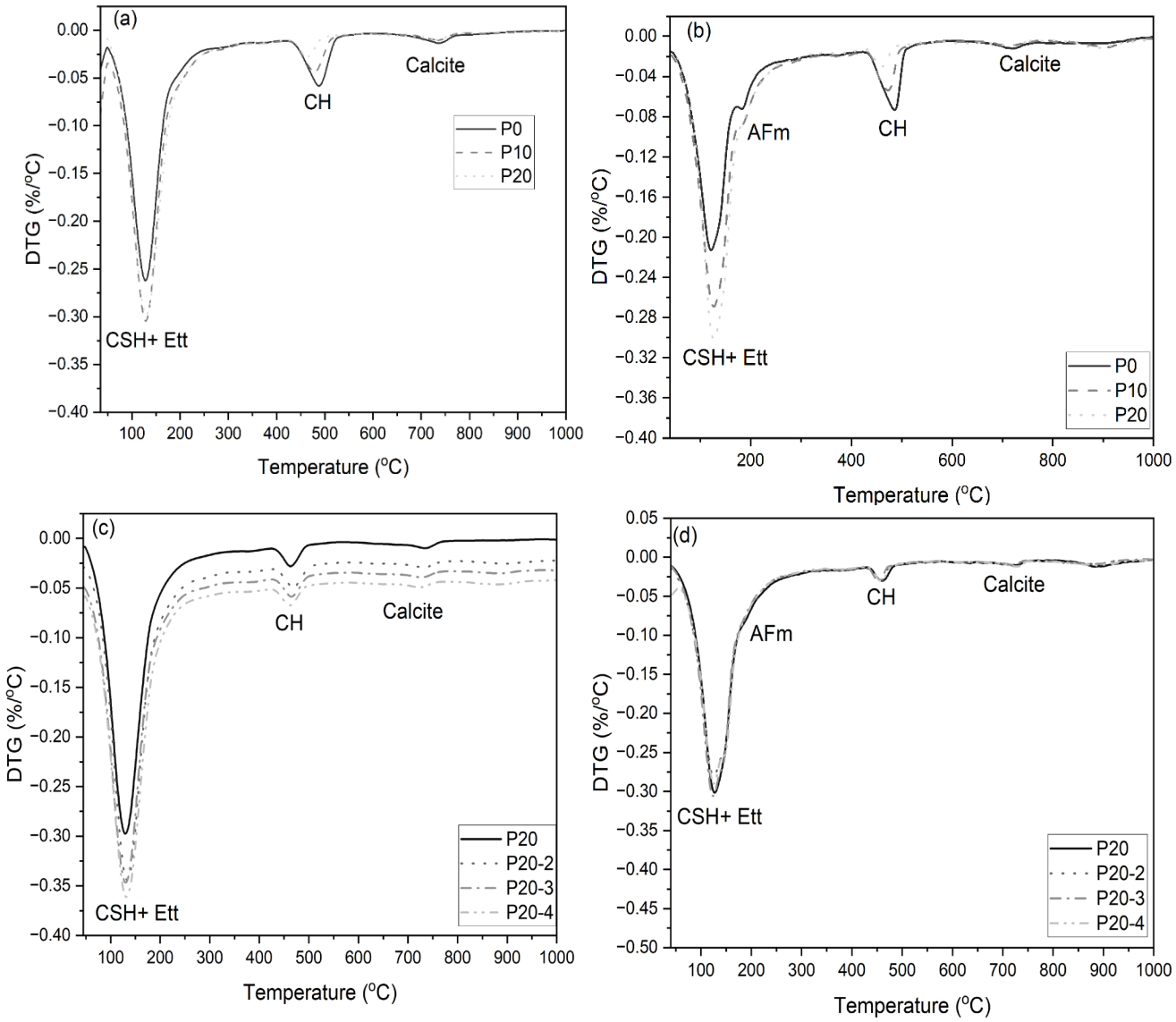

Figure 10 Portlandite content of cement paste at different silica replacement levels (a) and gypsum addition (0-4wt.%) for 20 wt.% silica

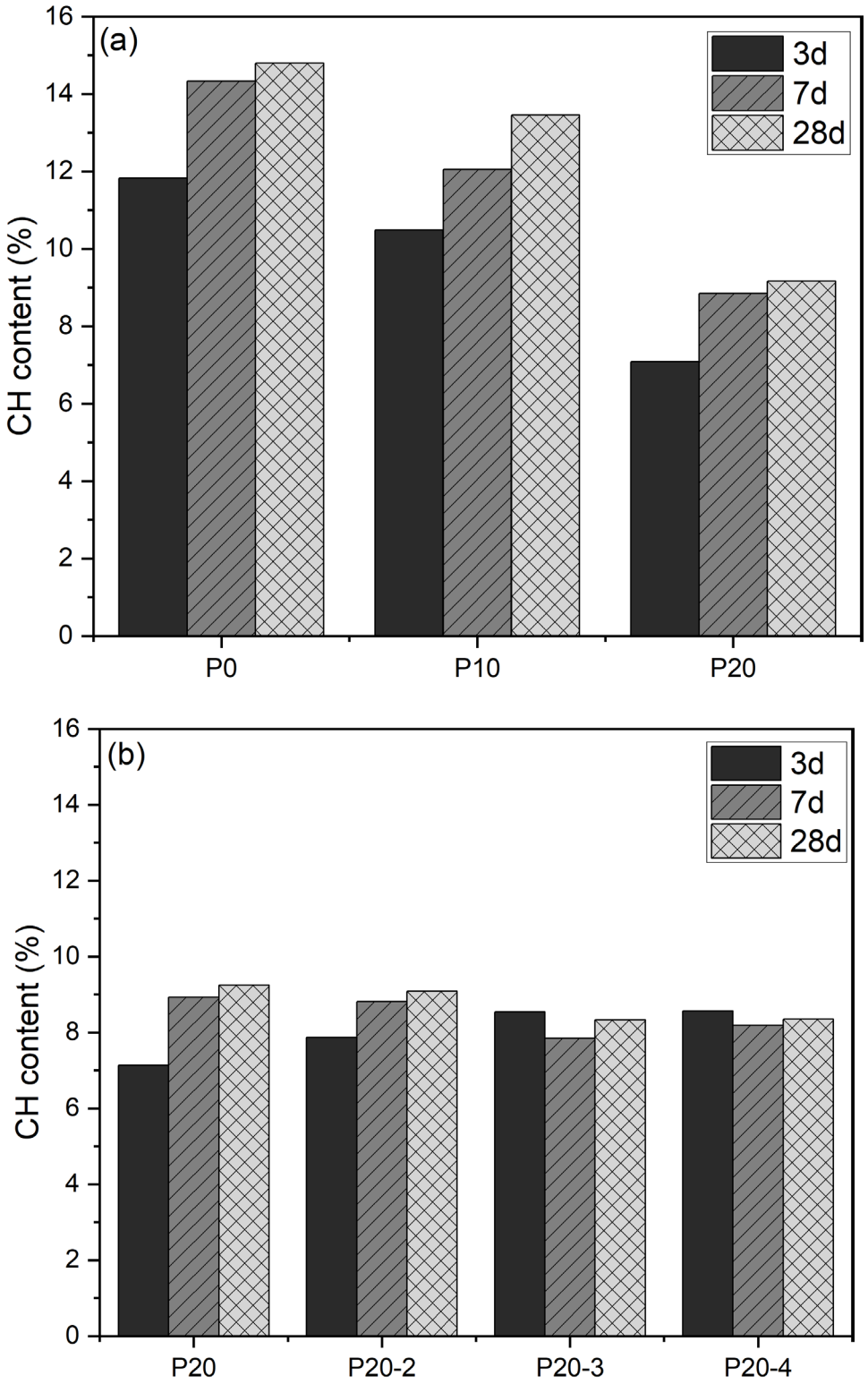

Influence of silica on water demand and workability

Fig 11 shows the evolution of the void ratio and solid concentration, also known as the packing behaviour, determined using the wet packing method. As developed by the particle packing theory, the water added for mortar preparation aims to first fill the voids between the particles, with the excess helping to form a workable mix [16,17]. The water demand corresponds to the minimum amount of water required to obtain a homogenous paste, as below this threshold the mixture is considered dry. For cement paste, the value of the packing density was found to be 0.578, equal to the highest solids concentration, corresponding to a W/CM volume ratio of 0.63 (0.20 in mass ratio). When cement is replaced by 30 wt.% silica the value of the packing density is significantly reduced to 0.363, corresponding to a W/CM volume ratio of 1.52, and a 0.55 in mass ratio. This means that more water is needed to fill the voids between particles, due to the higher SSA of the silica. Further, the water needed to produce a workable paste is also higher, which might induce some structural impairment. From this observation, the replacement level for preparing mortar was limited at 40 wt.% and the optimum W/CM (mass) to produce a workable mortar was 0.63 (1- Ø). Table 6 reports the data of the flow test of the mortar prepared with a W/CM mass ratio of 0.63. The control sample M0 had a flow of 162 mm and this decreased to 100 mm with 40wt.% silica replacement. The addition of gypsum to the mix design slightly improves the flowability up to 111.28 mm because of dilution effects, as previously described.

Figure 11 Packing behavior of the cementitious materials (a) OPC and (b) OPC+30wt.% silica

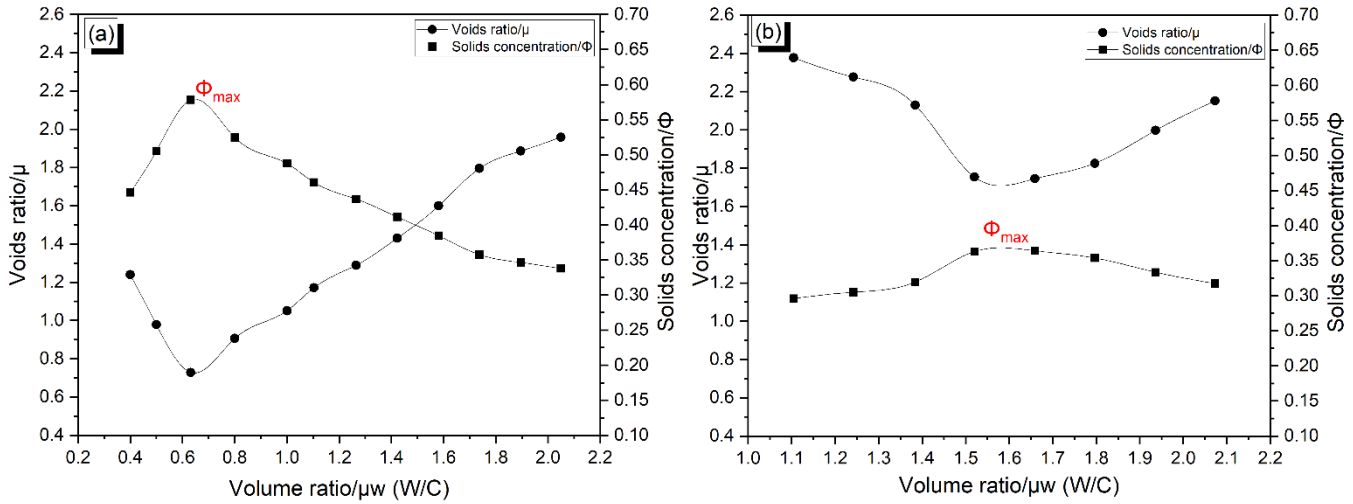

Table 6 Flow test results of mortar samples at W/CM mass ratio 0.63

Sample ID	M0	M10	M20	M40	M20-2	M20-3	M20-4
Flow (mm)	162.99	122.32	108.45	100.9	99.87	109.55	111.28
Std	±1.89	±0.27	±1.03	±0.7	±0.19	±1.56	±0.44

Compressive strength

The influence of silica and the gypsum addition for 20wt.% silica on compressive strength evolution is shown in Fig 12 and 13 respectively. In general, the compressive strength increases with the age of the sample. At an early age (3 and 7 days), the blended cement mortars developed a lower compressive strength than the control M0 (Fig 12a). After 7 days the compressive strength of blended cement mortars increases significantly with the silica content up to 20 wt.% where it is comparable to control at 28 days and higher at 90 days. However, 40 wt.% replacement, leads to a significant compressive strength loss at all ages. The effect of silica on strength evolution can be explained by the reaction mechanism prevailing at early age and late age. The dilution effect of silica likely controls the reaction mechanism of blended cement at an early age, which explains the low compressive strength despite the comparable or higher degree of hydration at 3 and 7 days with cement mortar. Indeed, the rapid formation of C-S-H due to the dilution effect accelerates the sulfate depletion by its sorption onto C-S-H gel. This also accelerates the aluminate reaction and hinders further C3S reaction. This can also explain the strength loss with a higher replacement level (40wt.%) where no portlandite is identified from 7 days probably because of the limited hydration of silicate phases. When compared to other silica-rich SCMs such as waste glass powder and rice hush ash it was observed in the literature that up to 20wt.% glass powder of cement replacement leads to a lower strength development at any age of replacement because of the predominance of the dilution effect over the pozzolanic reaction [18]. High early-age strength was achieved with rice hush ash-based blended cement at any age as a consequence of the simultaneous dilution and pozzolanic reaction [19]. Thus the rapid strength increase of blended cement mortar after 7 days can be ascribed to the contribution of the pozzolanic reaction as the dominant mechanism. The addition of extra sulfate from gypsum helps to correct the reaction mechanism at an early age by delaying the aluminate reaction and improving both the C3S and pozzolanic reaction. Consequently, the 3 and 7-day compressive strength of samples with extra gypsum are significantly improved (Fig 13). These changes at early age strength can be correlated with the calorimetry results which showed enhanced hydration of the C3S. It also agrees with the improved flowability because of the delayed aluminate hydration. However, the compressive strength at late age 28 and 90 dys does not change considerably with increased gypsum content (Fig 13). This confirms the little variation in CH content on those samples (M20-2 to M20-4) and indicate their limited contribution to promoting the pozzolanic reaction beyond 7 days as discussed previously.

Figure 12 Compressive strength evolution of mortar samples with different silica content

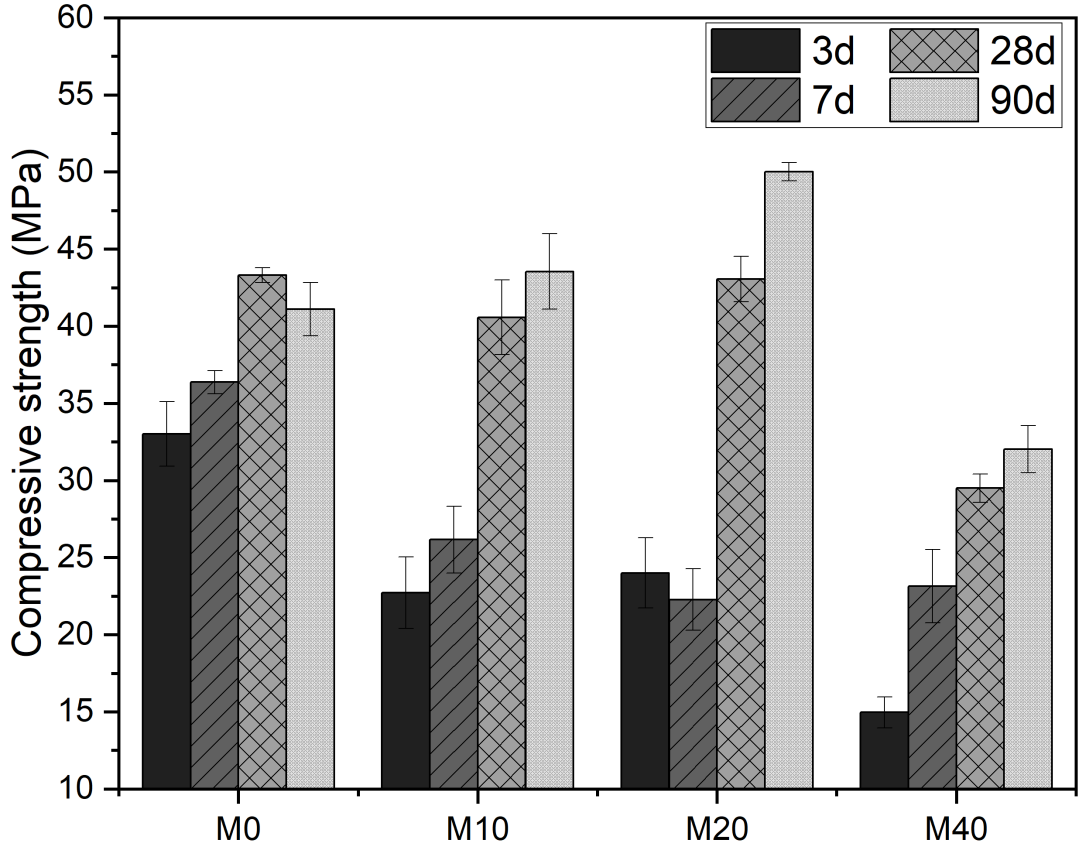

Figure 13 Compressive strength evolution of mortar samples with varying additional gypsum content for 20wt.% silica replacement.

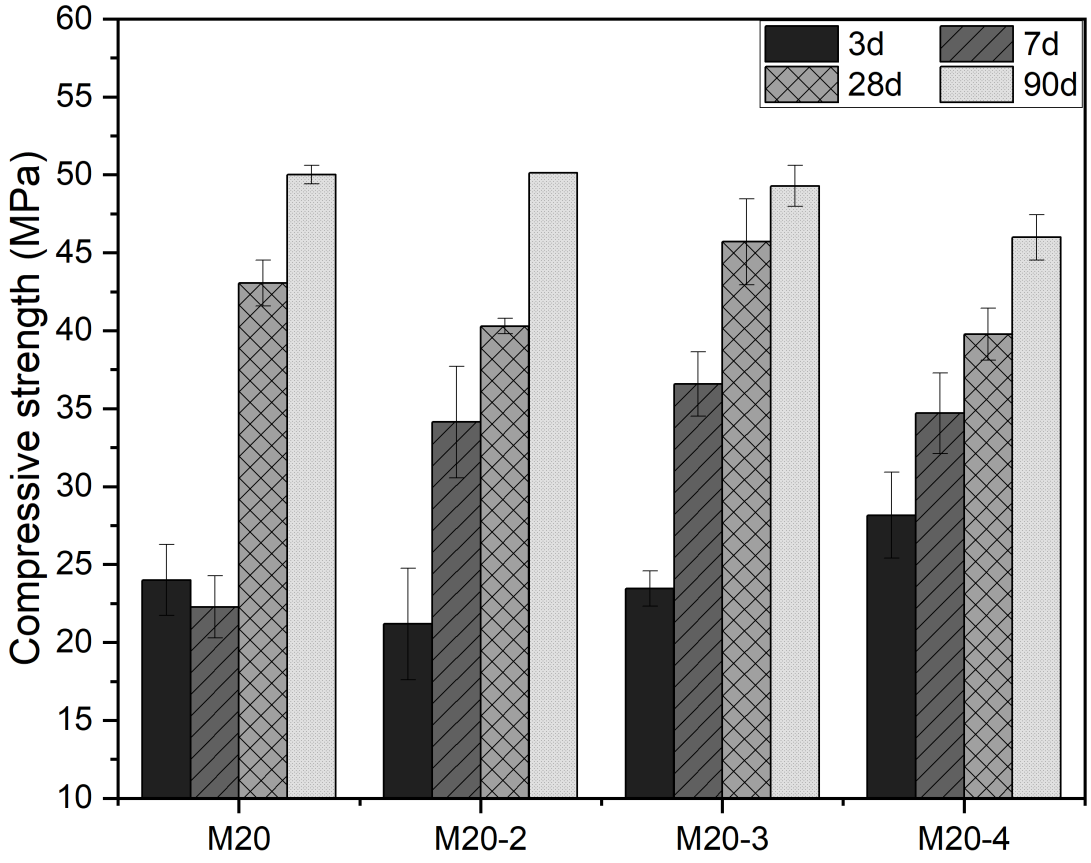

Conclusions

The reactivity of olivine-derived silica as SCM in blended cement is reported. The work has discussed the interactions of silica with cement hydration mechanisms, and the influence on strength development. The main findings are summarized as follows:

Olivine-derived silica can be classified as a suitable SCM. However, the high specific surface area increases water demand and makes it difficult to achieve a high replacement level without compromising workability and strength development. The high specific surface area of silica increases the water demand and significantly reduces the workability from 163 mm for control portland cement mortar to 100mm for blended cement mortar with up to 40wt.% silica at a w/c mass ratio of 0.63. The addition of extra gypsum is required to improve the workability of blended cement with silica.

The reaction of silica modifies the phase assemblage by improving the formation of hemicarbonate and monosulfate with silica content. Whereas the monocarbonate and monosulfate are promoted with the addition of gypsum.

The addition of APS promoted the dilution effect at an early age and rapid sulfate depletion with compressive strength not exceeding 25 MPa at 7 days. Beyond this age, the pozzolanic reaction takes over and improves the compressive that reaches 50 MPa at 90 days against 43 MPa for the control Portland cement mortar. Up to 4wt.% extra gypsum promoted both dilution and pozzolanic reaction and significantly enhanced the early age compressive strength to the level of control portland cement mortar.

Up to 20wt.% silica content is acceptable to achieve comparable or higher compressive strength to reference Portland cement at the same water-to-cement ratio.

References

[1] ASTM C1897-20, Standard Test Methods for Measuring the Reactivity of Supplementary Cementitious Materials by Isothermal Calorimetry and Bound Water Measurements, ASTM Int. West Conshohocken, PA. 04 (2020) 7–11. https://doi.org/10.1520/C1897-20.2.

[2] H.H.C. Wong, A.K.H. Kwan, Packing density of cementitious materials: Part 1-measurement using a wet packing method, Mater. Struct. Constr. 41 (2008) 689–701. https://doi.org/10.1617/s11527-007-9274-5.

[3] A.K.H. Kwan, H.H.C. Wong, Packing density of cementitious materials: Part 2-packing and flow of OPC + PFA + CSF, Mater. Struct. Constr. 41 (2008) 773–784. https://doi.org/10.1617/s11527-007-9281-6.

[4] D. Londono-Zuluaga, A. Gholizadeh-Vayghan, F. Winnefeld, F. Avet, M. Ben Haha, S.A. Bernal, Ö. Cizer, M. Cyr, S. Dolenec, P. Durdzinski, J. Haufe, D. Hooton, S. Kamali-Bernard, X. Li, A.T.M. Marsh, M. Marroccoli, M. Mrak, Y. Muy, C. Patapy, M. Pedersen, S. Sabio, S. Schulze, R. Snellings, A. Telesca, A. Vollpracht, G. Ye, S. Zhang, K.L. Scrivener, Report of RILEM TC 267-TRM phase 3: validation of the R3 reactivity test across a wide range of materials, Mater. Struct. 55 (2022). https://doi.org/10.1617/s11527-022-01947-3.

[5] P. Suraneni, J. Weiss, Examining the pozzolanicity of supplementary cementitious materials using isothermal calorimetry and thermogravimetric analysis, Cem. Concr. Compos. 83 (2017) 273–278. https://doi.org/10.1016/j.cemconcomp.2017.07.009.

[6] J. Yoon, K. Jafari, R. Tokpatayeva, S. Peethamparan, J. Olek, F. Rajabipour, Characterization and quantification of the pozzolanic reactivity of natural and non-conventional pozzolans, Cem. Concr. Compos. 133 (2022) 104708. https://doi.org/10.1016/j.cemconcomp.2022.104708.

[7] R. Snellings, D. Londoño-Zuluaga, K. Scrivener, Interlaboratory Test Program to Determine the Precision of the R3 Test Method (ASTM C1897-20) for Measuring Reactivity of Supplementary Cementitious Materials, Adv. Civ. Eng. Mater. 11 (2022). https://doi.org/10.1520/ACEM20220023.

[8] H.F.W. Taylor, Cement chemistry, 2nd ed., Thomas Telford Publishing, London, 1997. https://doi.org/10.1680/cc.25929.

[9] O. Canbek, C. Szeto, N.R. Washburn, K.E. Kurtis, A quantitative approach to determining sulfate balance for LC3, Cement. 12 (2023) 100063. https://doi.org/10.1016/j.cement.2023.100063.

[10] F. Zunino, K. Scrivener, The influence of the filler effect on the sulfate requirement of blended cements, Cem. Concr. Res. 126 (2019) 105918. https://doi.org/10.1016/j.cemconres.2019.105918.

[11] K. Scrivener, F. Avet, H. Maraghechi, F. Zunino, J. Ston, W. Hanpongpun, A. Favier, Impacting factors and properties of limestone calcined clay cements (LC3), Green Mater. 7 (2018) 3–14. https://doi.org/10.1680/jgrma.18.00029.

[12] M. Rubens, S. Andrade, B. Walkley, A. Paula, Exploring sulfate optimization techniques in Limestone Calcined Clay Cements (LC 3): limitations and insights, Cem. Concr. Res. 175 (2024) 107375. https://doi.org/10.1016/j.cemconres.2023.107375.

[13] S. Adu-Amankwah, L. Black, J. Skocek, M. Ben Haha, M. Zajac, Effect of sulfate additions on hydration and performance of ternary slag-limestone composite cements, Constr. Build. Mater. 164 (2018) 451–462. https://doi.org/10.1016/j.conbuildmat.2017.12.165.

[14] N. Raza, W. Raza, S. Madeddu, H. Agbe, R. V. Kumar, K.H. Kim, Synthesis and characterization of amorphous precipitated silica from alkaline dissolution of olivine, RSC Adv. 8 (2018) 32651–32658. https://doi.org/10.1039/c8ra06257a.

[15] K. Scrivener, R. Snellings, B. Lothenbach, A practical guide to microstructural analysis of cementitious materials, CCR Press, 2016. https://doi.org/10.1201/b19074.

[16] X. Chateau, Particle packing and the rheology of concrete, Underst. Rheol. Concr. (2012) 117–143. https://doi.org/10.1533/9780857095282.2.117.

[17] I. Mehdipour, K.H. Khayat, Effect of particle-size distribution and specific surface area of different binder systems on packing density and flow characteristics of cement paste, Cem. Concr. Compos. 78 (2017) 120–131. https://doi.org/10.1016/j.cemconcomp.2017.01.005.

[18] M. Mejdi, W. Wilson, M. Saillio, T. Chaussadent, L. Divet, A. Tagnit-Hamou, Hydration and microstructure of glass powder cement pastes – A multi-technique investigation, Cem. Concr. Res. 151 (2022). https://doi.org/10.1016/j.cemconres.2021.106610.

[19] F. Zunino, M. Lopez, Decoupling the physical and chemical effects of supplementary cementitious materials on strength and permeability: A multi-level approach, Cem. Concr. Compos. 65 (2016) 19–28. https://doi.org/10.1016/j.cemconcomp.2015.10.003.

If you need a version of this document in a more accessible format, please email alt.formats@energysecurity.gov.uk. Please tell us what format you need. It will help us if you say what assistive technology you use.